

# Anionic Polymerization of (Meth)acrylates in the Presence of Tetraalkylammonium Halide–Trialkyl Aluminum Complexes in Toluene. 3. Kinetic Investigations on Primary Acrylates<sup>†</sup>

Bardo Schmitt and Axel H. E. Müller<sup>\*,‡</sup>

Institut für Physikalische Chemie, Universität Mainz, Welterweg 15, D-55099 Mainz, Germany

Received September 15, 1999; Revised Manuscript Received December 29, 2000

**ABSTRACT:** The polymerization of *n*-butyl acrylate initiated by ester enolates in the presence of tetraalkylammonium halide–trialkylaluminum complexes,  $R_4N[Al_nR'_3X]$  ( $n = 1, 2$ ), in toluene has a controlled character at  $-78\text{ }^\circ\text{C}$  only for selected combinations of the complex. Quantitative monomer conversions are usually reached with  $Me_4N[Al_nBu'_3nCl]$  leading to polymers with narrow molecular weight distributions ( $M_w/M_n < 1.2$ ). Kinetic investigations show a complex mechanism of the polymerization, implying an equilibrium between at least two active species. Besides, various acrylate homopolymers and block copolymers (PMMA-*b*-polyacrylate) can be synthesized with this new initiating system.

## Introduction

Recently, we investigated the anionic polymerization of (meth)acrylates in the presence of tetraalkylammonium–trialkylaluminum 1:2 complexes  $NR_4[Al_2R'_6X]$  in toluene.<sup>1–3</sup> The polymerization proceeds in a living and controlled manner for methyl methacrylate up to  $0\text{ }^\circ\text{C}$ . Furthermore, quantitative monomer conversions are usually observed, and the resulting polymers have narrow molecular weight distributions. The reaction of MMA follows first-order kinetics with respect to initial concentrations of initiator, monomer and complex,<sup>3</sup> but at low concentrations of the complex, curved first-order time–conversion plots are found, and the polymers are initially bimodal. Thus, the mechanism of the reaction is rather complex, and we assume an equilibrium between at least two active species of different reactivity. Multinuclear NMR and quantum-chemical investigations on model compounds (ester enolates) made it possible to elucidate the structure of active species in polymerization of (meth)acrylates in the presence of tetraalkylammonium halide/aluminum alkyl complexes in nonpolar solvents.<sup>4</sup> Reaction of ethyl  $\alpha$ -lithioisobutyrate (EiBLi) with these complexes in equimolar amounts leads to the slow formation of different complexes,  $[EiBLi \cdot AlEt_3Cl]NMe_4$  and  $[EiBLi \cdot AlEt_3Cl \cdot AlEt_3]NMe_4$ . Because of an electron deficiency in the coordination sphere of lithium, these species tend to aggregate. Considering these NMR results, the dependence of the propagation rates on the size of both,  $NR_4^+$  and  $X^-$  in the complex obtained in the kinetics, can be explained by shifts of the equilibria between different active species.<sup>3</sup> In the real polymerization systems, coordination of ester groups of monomer and polymer also has to be taken into account. In fact, further NMR studies indicated a compensation of the electron deficiency by a model compound for the polymer ester groups, methyl pivalate.<sup>4</sup>

Earlier, we presented preliminary results of the anionic polymerization of primary acrylates (*n*-butyl

acrylate, *n*BuA, and 2-ethylhexyl acrylate, EHA) with lithiated initiators in the presence of tetraalkylammonium halide/aluminum alkyl complexes in toluene.<sup>1</sup> It was found that the complex between triisobutylaluminum and tetramethylammonium chloride supports a controlled polymerization at low temperatures ( $-78\text{ }^\circ\text{C}$ ). For tertiary acrylates (*tert*-butyl acrylate, tBuA) a controlled polymerization can even be achieved at  $-20\text{ }^\circ\text{C}$ .<sup>5</sup> In the present work we wish to enlighten the effect of tetraalkylammonium halide/aluminum alkyl complexes on kinetics and obtained molecular weight distributions in the anionic polymerization of *n*-butyl acrylate in toluene.

## Experimental Part

**Reagents.** Ethyl  $\alpha$ -lithioisobutyrate (EiBLi) was prepared according to the method of Lochmann and Lím.<sup>6</sup> Trimethyl aluminum ( $AlMe_3$ ), triethyl aluminum ( $AlEt_3$ ) and triisobutyl aluminum ( $AlBu'_3$ ) were purchased as 25 wt % solutions in toluene (Aldrich) and used as received. Tetraalkylammonium halides ( $Me_4NCl$ ,  $Et_4NCl$ ,  $Bu_4NCl$ , and  $Me_4NBr$ , Aldrich) were mixed with benzene and freeze-dried. *n*-Butyl acrylate (*n*BuA) and *tert*-butyl acrylate (tBuA, both BASF AG) were fractionated from  $CaH_2$  over a 1 m column filled with Sulzer packing at 45 mbar, stirred over  $CaH_2$ , degassed and distilled in a high vacuum. Toluene (BASF AG) was fractionated over a 1.5 m column, stirred twice over sodium/potassium alloy, degassed, and distilled in a high vacuum. Decane (internal standard for GC, Aldrich) were stirred over sodium/potassium alloy, degassed and distilled in a high vacuum.

**Kinetics.** All experiments were carried out in a stirred tank reactor under nitrogen atmosphere. First, the tetraalkylammonium halide/aluminum alkyl complex was stirred for 5 min in toluene at the later polymerization temperature. After introduction of the initiator, the solution was stirred for a further 5 min, and then the monomer was added. The polymerization was quenched with methanol/acetic acid (9:1 v/v), and monomer conversion was determined by GC using decane as internal standard. After evaporation of the solvent, the polymer was dissolved in benzene, filtered, and freeze-dried.

**GPC.** GPC was performed using THF as eluent at a flow rate of 1 mL/min. Detectors:  $2 \times$  JASCO–UVIDEC 100 III with variable wavelength and Bischoff RI detector 8110. Column set:  $2 \times 60\text{ cm}$ ,  $5\mu$  PSS SDV gel,  $100\text{ \AA}$ , and linear,  $10^2$ – $10^5\text{ \AA}$ . The PnBuA standards used for calibration had been synthesized in our laboratory and characterized by MALDI–TOF MS and GPC/MALLS measurements.

<sup>†</sup> Part 2. Cf. ref 4.

<sup>‡</sup> New address: Universität Bayreuth, Makromolekulare Chemie II, D-95440 Bayreuth, Germany. E-mail: axel.mueller@uni-bayreuth.de.

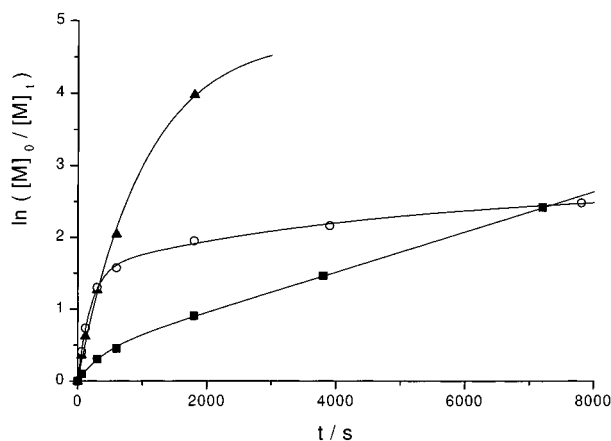


**Figure 1.** First-order time-conversion plots for the anionic polymerization of *n*BuA with EtBLi/NR<sub>4</sub>[Al<sub>2</sub>Bu<sub>6</sub>Cl] in toluene at -78 °C. Variation of R<sub>4</sub>NCl, R = (▲, run 3, Table S2) Bu, (○, run 4) Et, (■, run 5) Me. Conditions: [EtBLi]<sub>0</sub> = 4.9 × 10<sup>-4</sup> mol/L, [*n*BuA]<sub>0</sub> = 0.234 mol/L, [AlBu<sub>3</sub>] = 3.5 × 10<sup>-3</sup> mol/L, [R<sub>4</sub>NCl] = 1.7 × 10<sup>-3</sup> mol/L, and Al:N:Li = 7.1:3.5:1.

**MALDI-TOF MS.** Spectra were recorded with a Bruker Reflex mass spectrometer which is equipped with a nitrogen laser source delivering 3 ns pulses at  $\lambda = 337$  nm. 1,8,9-Trihydroxyanthracene was used as the matrix and potassium trifluoroacetate as the cationization agent.

## Results and Discussion

**Effect of Different Complexes NR<sub>4</sub>[Al<sub>2</sub>R<sub>6</sub>X].** According to Ziegler et al.<sup>7</sup> tetraalkylammonium halides give soluble complexes (NR<sub>4</sub>[Al<sub>n</sub>R<sub>3n</sub>X], *n* = 1, 2) with aluminum alkyls in toluene. Initiation with ester enolates in the presence of these complexes leads to a living and controlled polymerization of MMA. In contrast to MMA polymerization, it is more difficult to obtain a controlled polymerization of primary acrylates in the presence of tetraalkylammonium halide/aluminum alkyl complexes; not all complex combinations lead to a gain in reaction control. Performing the polymerization with NMe<sub>4</sub>Cl in combination with different aluminum alkyls, high monomer conversion and polymers with narrow molecular weight distributions are only obtained in the presence of triisobutylaluminum (see Figure 1, run 3 and Supporting Information, Figure S1 and Table S1). However, we found a kinked first-order time-conversion plot. By using the initial slope of the first-order time-conversion plot,  $k_{app}$ , we can calculate  $\bar{k}_p = k_{app}/[P^*]$ .  $\bar{k}_p$  is only an apparent constant of polymerization, since it depends on the initial concentration and nature of the NR<sub>4</sub>[Al<sub>n</sub>R<sub>3n</sub>X] complex.<sup>1,3</sup> It is found that the effect of the size of the aluminum alkyl on  $\bar{k}_p$  in the polymerization of acrylates is not very pronounced. Significant effects on the rates of polymerization are observed, when varying NR<sub>4</sub><sup>+</sup> and X<sup>-</sup>, which will be described in the next few paragraphs.

Increasing the size of the tetraalkylammonium ion leads to a higher initial rate of propagation (see Figure 1 and Table S2). Indeed, in agreement with studies on the structure of the active species in MMA polymerization obtained from quantum-chemical calculations,<sup>4</sup> one would expect that the radius of the tetraalkylammonium gegenion has a significant effect on the interionic distance to the carbanion and thus on the reactivity of the active chain end (Scheme 1). Consequently, a larger tetraalkylammonium ion should lead to a higher rate of polymerization, which is indeed observed. Nevertheless, control of the polymerization is lost for

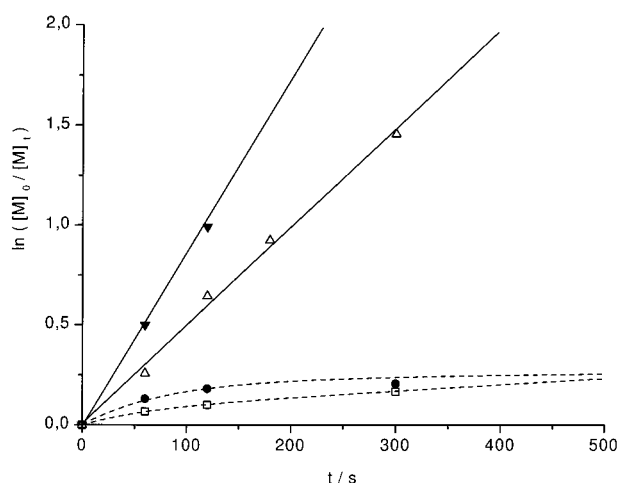
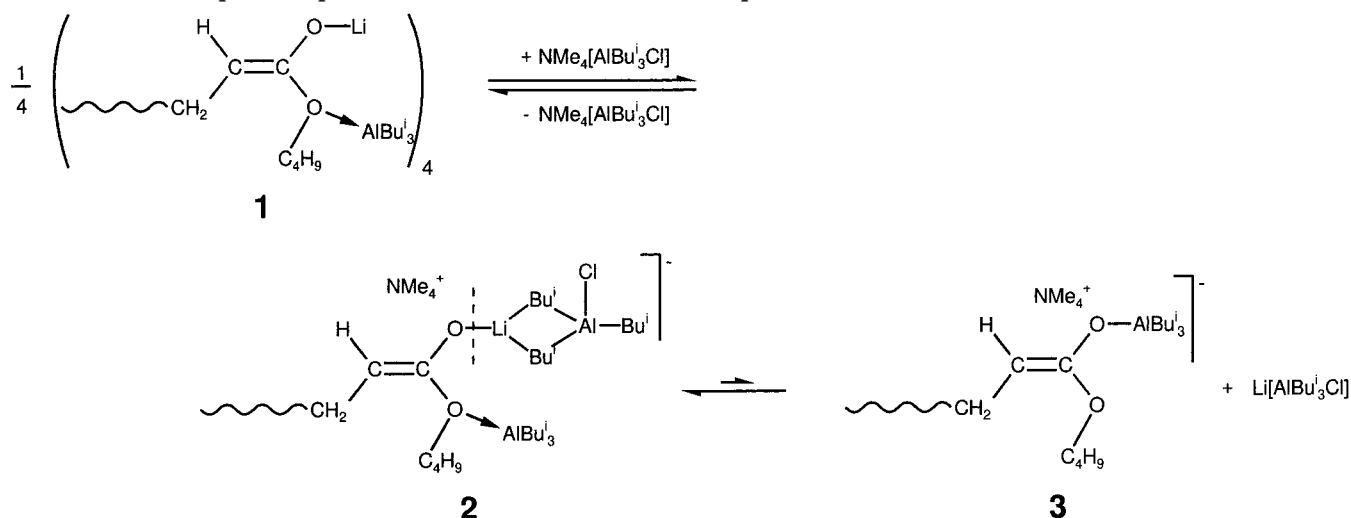
bulkier tetraalkylammonium ions and the molecular weight distribution of the obtained polymers broadens (Table S2).

It is found that the initial rate of propagation increases also with decreasing radius of the halide (Br<sup>-</sup> < Cl<sup>-</sup>). This effect was also observed and discussed in the polymerization of MMA.<sup>3</sup> It could be explained with a shift in the equilibrium  $1 \rightleftharpoons 2$  toward the more reactive species **2** (Scheme 1). The higher reactivity of the  $\alpha$ -carbon is due to a compensation of the electron deficiency at the lithium, when the ammonium complex coordinates. To explain the shift in the equilibrium, it was supposed that its position and/or the degree of association of the active chains depend on their degree of polymerization. It has also been proposed that the active species **2** is able to dissociate into a very reactive ammonium enol aluminate complex **3** and the complex Li[AlR<sub>3</sub>X]. The heat of formation of Li[AlR<sub>3</sub>X] increases as the radius of the halide decreases,<sup>7</sup> so the higher initial rate of propagation for chloride could be explained by a shift in the equilibrium toward the active species **3**. Nevertheless, quantum-chemical calculations on model compounds provide a very high heat of formation for ammonium enolates (heat of formation  $\Delta E = +76.0$  kJ/mol for the model compound EtBLi,<sup>4</sup> analogous to Scheme 1, reaction  $2 \rightarrow 3$ ). Therefore, the equilibrium should lie nearly exclusively on the side of the less reactive but more stable species **2**. Again, the polymerization loses its controlled character in the case of bromide, as shown by incomplete monomer conversion and broad molecular weight distributions (see Figure S3, Table S2).

One can conclude that the polymerization only proceeds in a controlled manner, if NMe<sub>4</sub>[Al<sub>2</sub>Bu<sub>6</sub>Cl] is used. Thus, we describe now how this complex affects the kinetics and molecular weight distributions of the anionic polymerization.

**Effect of Complexes NMe<sub>4</sub>[AlBu<sub>3</sub>Cl] and NMe<sub>4</sub>[Al<sub>2</sub>Bu<sub>6</sub>Cl].** Compared to the anionic polymerization of *n*BuA with EtBLi/AlBu<sub>3</sub> in pure toluene or a toluene/methyl pivalate mixed solvent (72/28 v/v), the initial rate of propagation is significantly higher when we use EtBLi in the presence of NMe<sub>4</sub>[AlBu<sub>3</sub>Cl] and NMe<sub>4</sub>[Al<sub>2</sub>Bu<sub>6</sub>Cl] in toluene (cf. Figure 2). A precipitation of a polymer gel, which was observed in the EtBLi/AlBu<sub>3</sub> system,<sup>8</sup> cannot be observed. Furthermore, the apparent rate of polymerization for NMe<sub>4</sub>[Al<sub>2</sub>Bu<sub>6</sub>Cl] is higher than for NMe<sub>4</sub>[AlBu<sub>3</sub>Cl] and the polymers have narrower molecular weight distributions. However, we now find linear first-order time-conversion plots in the presence of both complexes. As the plots of the number-average degree of polymerization vs monomer conversion for the polymerization shown in Figure 3 are also linear, transfer reactions can be excluded.

**Effect of Initial Concentration of Initiator.** Surprisingly, we again observe kinked first-order time-conversion plots at different initial concentrations of initiator (Figure 4). Especially in the case of [EtBLi]<sub>0</sub> = 0.98 × 10<sup>-4</sup> mol/L (run 12), we obtain different results in this experiment compared to the one in Figure 2 (run 10), although the complex concentration differs only slightly. Thus, we assume that the polymerization system is very sensitive to changes in concentrations of the components, leading to a shift of equilibria between different active species. Nevertheless, the reaction follows first-order kinetics with respect to initial concentration of initiator (see Figure 5) and monomer<sup>9</sup>

**Scheme 1. Proposed Equilibria between Different Active Species (for 2 and 3, Dimeric Structures Omitted)**

**Figure 2.** First-order time-conversion plots for the anionic polymerization of *n*BuA with EiBLi in the presence of different additives in toluene at  $-78\text{ }^{\circ}\text{C}$ : ( $\square$ , run 8, Table S3)  $\text{AlBu}_3$ ,  $\text{Al:N:Li} = 3.3:0:1$ ; ( $\bullet$ , run 9)  $\text{AlBu}_3/\text{MPiv}$ ,  $\text{Al:N:Li} = 3.6:0:1$ ; ( $\triangle$ , run 11)  $\text{NMe}_4[\text{AlBu}_3\text{Cl}]$ ,  $\text{Al:N:Li} = 3.7:1.8:1$ ; ( $\blacktriangle$ , run 10)  $\text{NR}_4[\text{Al}_2\text{Bu}_6\text{Cl}]$ ,  $\text{Al:N:Li} = 1.8:1.7:1$ . Conditions:  $[\text{EiBLi}]_0 \approx 1.0 \times 10^{-3} \text{ mol/L}$ ,  $[\text{nBuA}]_0 = 0.234 \text{ mol/L}$ , and  $[\text{MPiv}] = 2.1 \text{ mol/L}$ .

in both the initial and final rates of polymerization. It seems therefore reasonable to assume an equilibrium between various active species of different reactivity.

**Effect of the Complex Concentration.** The first-order time-conversion plots are only linear when a high concentration of  $\text{NMe}_4[\text{Al}_2\text{Bu}_6\text{Cl}]$  is used (Figure 6). Otherwise the plots show a kink, and we observe two apparent rate constants of propagation. A bilogarithmic plot of both initial and final rate constants of propagation vs complex concentration shows that the polymerization follows first-order kinetics with respect to complex concentration (Figure S4). Nevertheless, the kink cannot be explained by the increase of the rate of polymerization caused by higher complex concentration, nor by a shift in the equilibrium  $1 \rightleftharpoons 2$  discussed in Scheme 1. Therefore, we suppose that an equilibrium exists between different active species, the position of which and the degree of aggregation of the living chains depending on the degree of polymerization. Polydispersity indices decrease with increasing complex concentration.

In some cases the initiator efficiency,  $f = P_{n,\text{th}}/P_{n,\text{exp}}$ , is surprisingly high, increasing with increasing concen-

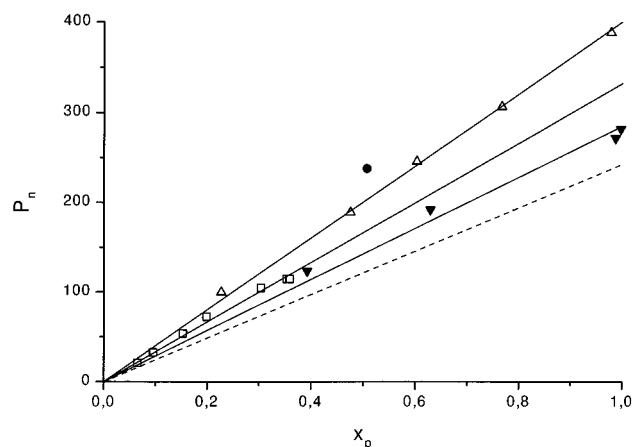


**Figure 3.** Number-average degree of polymerization vs monomer conversion for the anionic polymerization of *n*BuA with EiBLi in the presence of different additives in toluene at  $-78\text{ }^{\circ}\text{C}$ : ( $\square$ , run 8)  $\text{AlBu}_3$ ,  $\text{Al:N:Li} = 3.3:0:1$ ; ( $\bullet$ , run 9)  $\text{AlBu}_3/\text{MPiv}$ ,  $\text{Al:N:Li} = 3.6:0:1$ ; ( $\triangle$ , run 11)  $\text{NMe}_4[\text{AlBu}_3\text{Cl}]$ ,  $\text{Al:N:Li} = 3.7:1.8:1$ ; ( $\blacktriangle$ , run 10)  $\text{NMe}_4[\text{Al}_2\text{Bu}_6\text{Cl}]$ ,  $\text{Al:N:Li} = 1.8:1.7:1$ . For reaction conditions, see Figure 2.

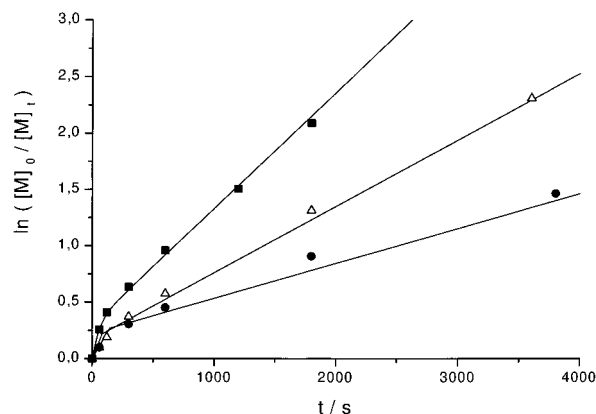


**Figure 4.** First-order time-conversion plots for the anionic polymerization of *n*BuA with EiBLi/ $\text{NMe}_4[\text{Al}_2\text{Bu}_6\text{Cl}]$  for different initiator concentrations in toluene at  $-78\text{ }^{\circ}\text{C}$ .  $[\text{EiBLi}]_0 = (\bullet$ , run 3, Table S4) 4.9, ( $\triangle$ , run 12) 9.8, ( $\blacksquare$ , run 13)  $23.3 \times 10^{-4} \text{ mol/L}$ . Conditions:  $[\text{nBuA}]_0 = 0.234 \text{ mol/L}$ ,  $[\text{AlBu}_3] = 3.5 \times 10^{-3} \text{ mol/L}$ , and  $[\text{Me}_4\text{NCl}] = 1.7 \times 10^{-3} \text{ mol/L}$ .

tration of  $\text{NMe}_4[\text{Al}_3\text{Bu}_6\text{Cl}]$  and reaching values up to  $f = 4.3$ . Transfer reactions can be excluded, because the plot of the number-average degree of polymerization vs

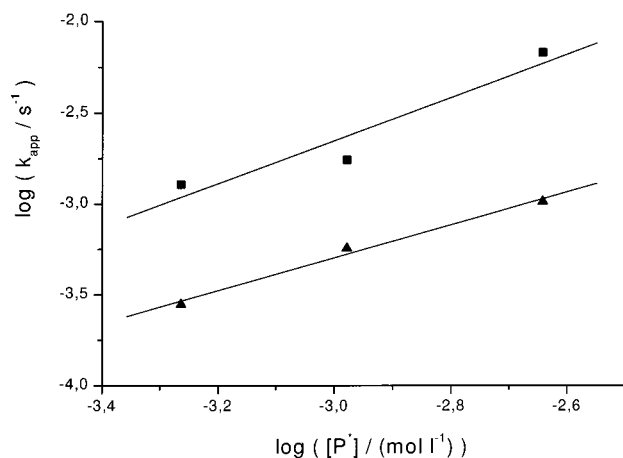


**Figure 5.** Determination of the reaction order with respect to the concentration of the initial concentration of initiator. Initial apparent rate constant (■), slope  $1.2 \pm 0.4$ ; final apparent rate constant (▲), slope  $0.9 \pm 0.1$ .

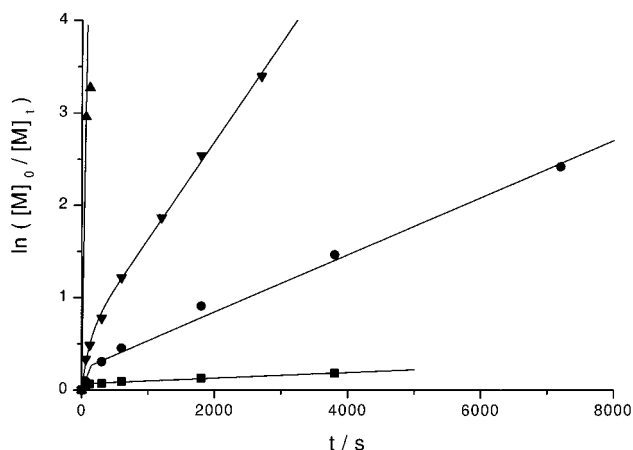


**Figure 6.** First-order time-conversion plots for the anionic polymerization of  $n$ BuA with  $\text{EtBLi}/\text{NMe}_4[\text{Al}_2\text{Bu}_6\text{Cl}]$  for different complex concentrations in toluene at  $-78^\circ\text{C}$ .  $[\text{AlBu}_3]/[\text{Me}_4\text{NCl}] =$  (■, run 14, Table S5) 0.72/0.36, (●, run 3) 3.5/1.7, (▼, run 6) 14.0/6.9, (▲, run 15)  $28.0/13.9 \times 10^{-3}$  mol/L. Conditions:  $[\text{EtBLi}]_0 = 4.9 \times 10^{-4}$  mol/L and  $[n\text{BuA}]_0 = 0.234$  mol/L.

the monomer concentration is linear in all cases. A reasonable explanation could be the initiation by the complex itself. Therefore, MALDI-TOF MS measurements were performed in order to elucidate the occurrence of side reactions. A MALDI-TOF mass spectrum of a polymer sample obtained from the polymerization in Figure 6 (Al:N = 14:6.9) shows several different end groups (Figure 7). Beside the expected, EiB-initiated polymer chain (x, residual mass 155 Da =  $m(\text{EiB}) + m(\text{H}) + m(\text{K}^+)$ ), a second one with the residual mass of 41 Da is observed. This might be due to an initiation by hydride ions (41 Da =  $m(\text{H}) + m(\text{H}) + m(\text{K}^+)$ ; see Scheme 2). The new active center could be stabilized by the dialkylaluminum halide. These findings are in agreement with those of the polymerization in the presence of cesium halide/trialkylaluminum complexes, where an initiation by the complex itself was observed.<sup>10</sup>

Additionally, we find a small extent of cyclic terminated polymer chains (EiB-initiated o, residual mass 81 Da =  $m(\text{EiB}) - m(\text{BuO}) + m(\text{K}^+)$ ; hydride-initiated v, residual mass 95 Da =  $m(\text{H}) + m(n\text{BuA}) - m(\text{BuO}) + m(\text{K}^+)$ ) and polymer chains with two cyclic  $\beta$ -ketoester

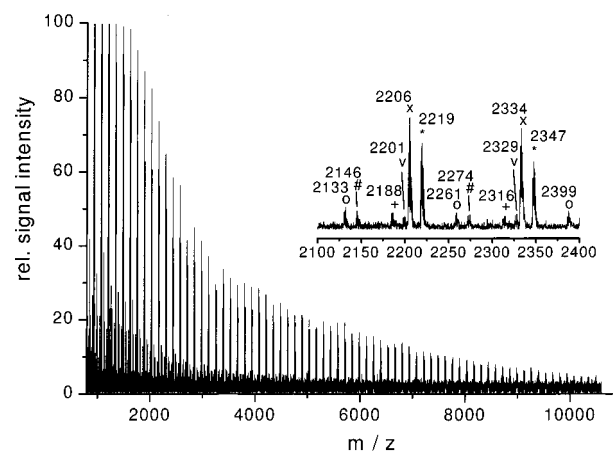


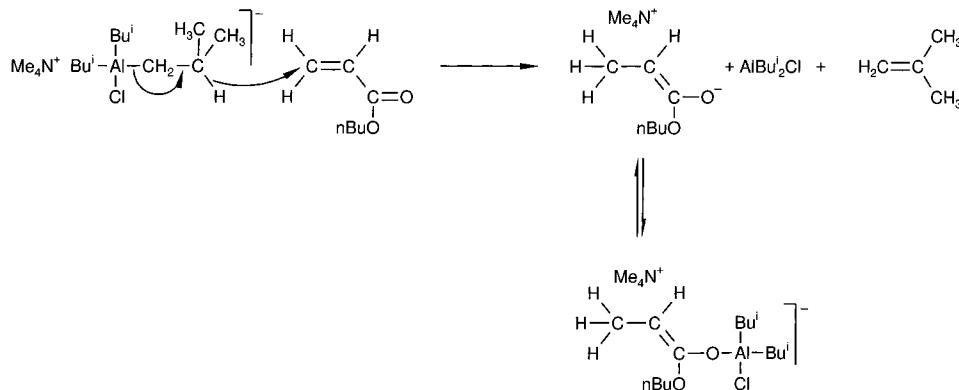
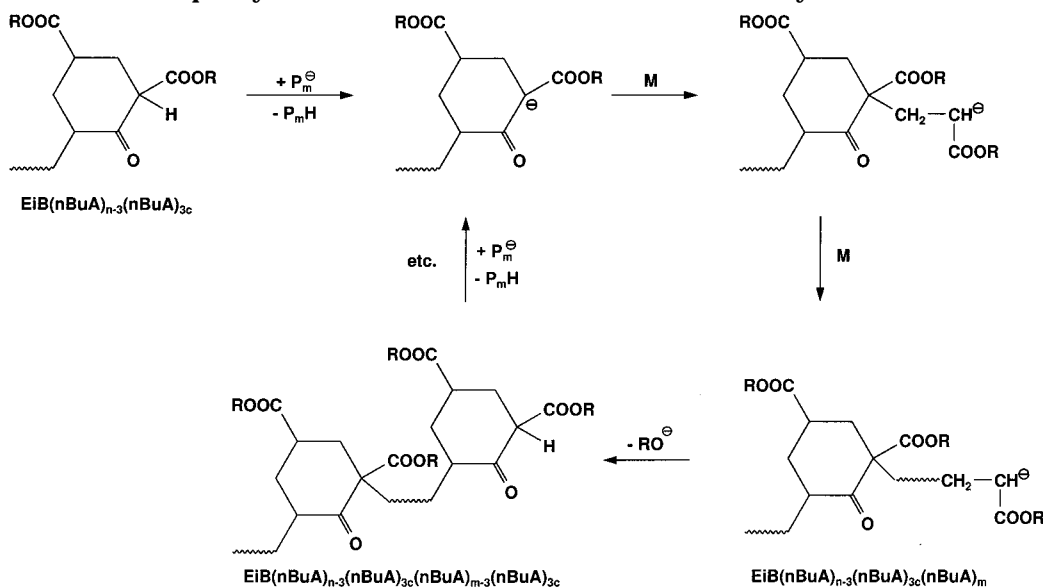
**Figure 7.** MALDI-TOF mass spectrum of PnBuA obtained in Figure 6 (▼, run 6) at 120 s. EiB-initiated polymer chains:  $m/z = xx155$  linear (x),  $xx81$  cyclic terminated (o), and  $xx135$  twice cyclic terminated (+). Hydride-initiated polymer chains:  $m/z = xx41$  linear (\*),  $xx95$  cyclic terminated (v), and  $xx149$  twice cyclic terminated (#). Repeat unit of all series: 128.2 Da. See also Scheme 3.

groups (EiB-initiated +, residual mass 135 Da =  $m(\text{EiB}) + m(n\text{BuA}) - 2m(\text{BuO}) - m(\text{H}) + m(\text{K}^+)$ ; hydride-initiated numbers, residual mass 149 Da =  $m(\text{H}) + m(n\text{BuA}) - 2m(\text{BuO}) - m(\text{H}) + m(\text{K}^+)$ ). We assume that after abstraction of an acidic proton and reinitiation a second cyclic termination reaction occurs (cf. Scheme 3). Nevertheless, polymer chains containing three or more cyclic  $\beta$ -ketoester groups and initiation by butoxide (residual mass 93 Da) cannot be detected.

**Temperature Dependence.** At temperatures higher than  $-78^\circ\text{C}$ , the time-conversion plots show a downward curvature and incomplete conversions, indicating the occurrence of termination (Figure 8). In GPC analysis we find significant UV absorption at  $\lambda = 260$  nm, which is characteristic for enolized cyclic  $\beta$ -ketoester end groups.<sup>11</sup> NMR investigations on model compounds at ambient temperature suggest that beside cyclization a second termination reaction is observed. Hofmann elimination and methylation were obtained by Bandermann et al.<sup>12,13</sup> in the polymerization of MMA in THF with tetrabutyl- and tetramethylammonium malonates, respectively. Thus, in conjunction with increasing back-biting termination, the molecular weight distributions of the obtained polymers broaden ( $M_w/M_n > 1.5$ ). The Arrhenius plot of the propagation rate constants, which can be determined from the initial slopes, is linear below  $-60^\circ\text{C}$ . At higher temperatures the rate constants cannot be determined exactly. We have shown above that the  $k_p$  values depend on the complex concentration. Consequently, regarding the complex mechanism and the sensitive equilibria between different active species, the values of the activation parameters must be apparent ones. They are determined from Figure 9 as  $E_a^{\text{app}} = (32.1 \pm 3.5)$  kJ/mol and  $\log A_{\text{app}} = 9.7 \pm 0.9$ . The calculated value of the activation energy is higher than those usually observed with various counterions and solvents. Activation energies between 17 and 23 kJ/mol are usually reported for  $\text{Li}^+$  and GTP in toluene.<sup>9,14,15</sup>

**Block Copolymerization.** Block copolymers, like PMMA-*b*-PtBuA and PMMA-*b*-PnBuA, with narrow molecular weight distributions can be synthesized via sequential monomer addition. As discussed before, reaction conditions are different for the polymerization



Scheme 2. Initiation of NBuA by Hydride Transfer from  $\text{Me}_4\text{N}[\text{Al}_2\text{Bu}_6\text{Cl}]$ Scheme 3. Multiple Cyclic Termination and Re-initiation in the Polymerization of NBuA<sup>a</sup>

<sup>a</sup>  $\text{P}_m$ , polymer chain; M, monomer;  $(n\text{BuA})_{n-3}$ , monomer units of the linear polymer chain;  $(n\text{BuA})_{3c}$ , cyclic terminated units of the polymer chain.

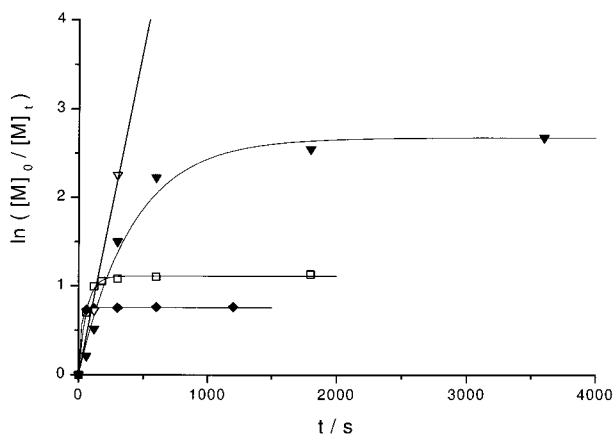


**Figure 8.** First-order time-conversion plots for the anionic polymerization of  $n\text{BuA}$  with  $\text{EiBLi}/\text{NMe}_4[\text{Al}_2\text{Bu}_6\text{Cl}]$  in toluene at  $-78$  ( $\nabla$ , run 15, Table S6),  $-70$  ( $\blacktriangledown$ , run 17),  $-60$  ( $\square$ , run 18), and  $-40$  ( $\blacklozenge$ , run 19). Conditions:  $[\text{EiBLi}]_0 = 4.9 \times 10^{-4}$  mol/L,  $[n\text{BuA}]_0 = 0.195$  mol/L,  $[\text{AlBu}_3]/[\text{Me}_4\text{NCl}] = 3.5/1.7 \times 10^{-3}$  mol/L, and  $\text{Al:N:Li} = 7.1:3.5:1$ .

of methacrylates and acrylates. Thus, the polymerization system must be optimized for each polymerization step. While using  $\text{EiBLi}/\text{NMe}_4[\text{Al}_2\text{Et}_6\text{Cl}]$  for synthesizing PMMA-*b*-PtBuA ( $M_{n,\text{app}} = 41\,000$ ,  $M_w/M_n = 1.1$ , blocking

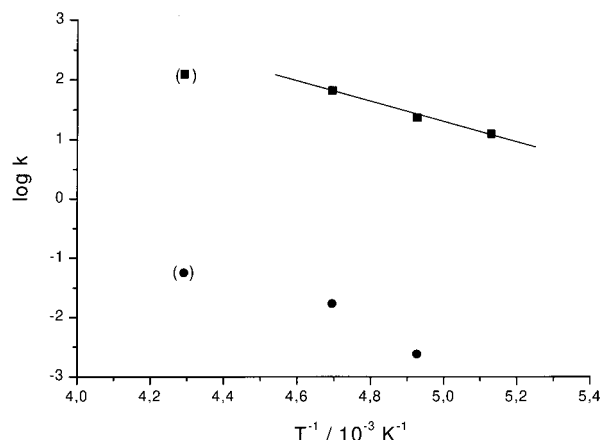


**Figure 9.** Arrhenius plot for the anionic polymerization of  $n\text{BuA}$  with  $\text{EiBLi}/\text{NMe}_4[\text{Al}_2\text{Bu}_6\text{Cl}]$  in toluene. Initial apparent rate constant  $k_p$ ,  $E_a^{\text{app}} = (32.1 \pm 3.5)$  kJ/mol,  $\log A_{\text{app}} = 9.7 \pm 0.9$  ( $\blacksquare$ ); apparent rate constant of termination,  $k_t$  ( $\bullet$ ).

efficiency  $f \approx 0.9$ ; Figure S5), the polymerization conditions for PMMA-*b*-PnBuA are changed. After MMA conversion is complete, excess  $\text{NMe}_4[\text{Al}_2\text{Bu}_6\text{Cl}]$  is added in order to gain reaction control in  $n\text{BuA}$  polymerization. However, even then the blocking efficiency does not exceed 90% (Figure 10). Thus, further optimization is

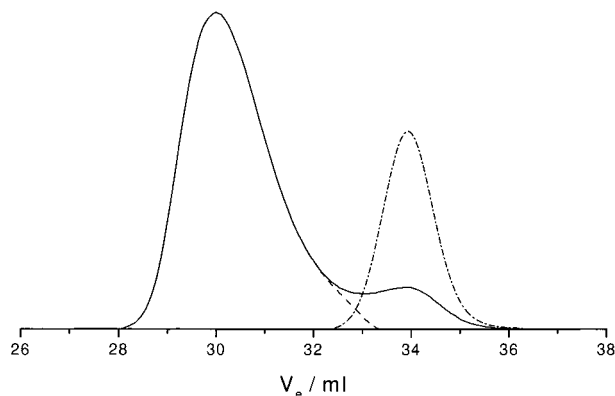


**Figure 10.** GPC eluogram of a PMMA-*b*-PnBuA (—) obtained with  $\text{EtBLi}/\text{NMe}_4[\text{Al}_2\text{Et}_6\text{Cl}]$  at  $-20^\circ\text{C}$  (MMA) and  $\text{NMe}_4[\text{Al}_2\text{Bu}_6\text{Cl}]$  ( $n\text{BuA}$ ) at  $-78^\circ\text{C}$ :  $M_{n,\text{app}} = 30\,000$ ,  $M_w/M_n = 1.3$  (---, without precursor); precursor,  $M_n = 5000$ ,  $M_w/M_n = 1.1$  (- · -); blocking efficiency,  $f \approx 0.8$ . Reaction conditions:  $[\text{EtBLi}]_0 = 4.6 \times 10^{-3}$  mol/L,  $[\text{MMA}]_0 = 0.23$  mol/L,  $[\text{AlEt}_3]/[\text{Me}_4\text{NCl}] = 4.8/4.4 \times 10^{-3}$  mol/L,  $[n\text{BuA}]_0 = 0.25$  mol/L, and  $[\text{AlBu}_3]/[\text{Me}_4\text{NCl}] = 7.0/6.8 \times 10^{-3}$  mol/L.

necessary to prepare block copolymers without residual precursor.

### Conclusions

The polymerization of  $n\text{BuA}$  with  $\text{EtBLi}$  in the presence of the  $\text{NMe}_4[\text{Al}_2\text{Bu}_6\text{Cl}]$  complex has a controlled character at  $-78^\circ\text{C}$ . The reaction follows first-order kinetics with respect to the initial concentrations of initiator, monomer, and complex. Changing reaction conditions often leads to curved time-conversion plots, which are not completely understood yet, while the polymerization always reaches full monomer conversion at  $-78^\circ\text{C}$ . The molecular weight distributions of the polymers obtained get very narrow for optimized reaction conditions ( $M_w/M_n < 1.1$ ). Nevertheless, the polymerization system is very sensitive to reaction conditions, presumably due to shifts in the position of equilibria between at least two active species of different reactivity. However, the polymerization loses its controlled character at higher temperatures when termination

reactions become dominant. The successful homopolymerization of several acrylates and the synthesis of block copolymers show the ability of this new initiating system in order to synthesize various polymer architectures.

**Acknowledgment.** We wish to thank Mrs. Nicole Gilbert and Mr. Peter Blumers for their very helpful hands. This work was supported by the Bundesministerium für Bildung, Wissenschaft, Forschung und Technologie and BASF AG, Ludwigshafen, Germany (Project No. 03N 3006 A5).

**Supporting Information Available:** Tables S1–S6, giving data for the effects of various additives, different initiator concentrations, and temperature on the polymerization, and Figures S1–S5, showing time-conversion plots, plots of polydispersity vs monomer conversion, determination of the reaction order, and a GPC eluogram. This material is available free of charge via the Internet at <http://pubs.acs.org>.

### References and Notes

- (1) Schlaad, H.; Schmitt, B.; Müller, A. H. E. *Angew. Chem.* **1998**, *110*, 1497; *Angew. Chem., Int. Ed. Engl.* **1998**, *37*, 1389.
- (2) Schlaad, H.; Schmitt, B.; Müller, A. H. E.; Jüngling, S.; Weiss, H. *Macromol. Symp.* **1998**, *132*, 293.
- (3) Schlaad, H.; Müller, A. H. E. *Macromolecules* **1998**, *31*, 7127.
- (4) Schmitt, B.; Schlaad, H.; Müller, A. H. E.; Mathiasch, B.; Steiger, S.; Weiss, H. *Macromolecules* **2000**, *33*, 2887.
- (5) Schlaad, H.; Dissertation, Universität Mainz 1997.
- (6) Lochmann, L.; Lim, D. *J. Organomet. Chem.* **1973**, *50*, 9.
- (7) Ziegler, K.; Köster, R.; Lehmkuhl, H.; Reinert, K. *Liebigs Ann. Chem.* **1960**, 629, 33.
- (8) Schmitt, B.; Schlaad, H.; Müller, A. H. E. *Macromolecules* **1998**, *31*, 1705.
- (9) Schmitt, B. Dissertation, Universität Mainz 1999.
- (10) Schmitt, B.; Stauf, W.; Müller, A. H. E. *Macromolecules* **2001**, *34*, in press; published on the Internet on Feb 14, 2001.
- (11) Janata, M.; Lochmann, L.; Müller, A. H. E. *Makromol. Chem.* **1990**, *191*, 2253.
- (12) Fieberg, A.; Broska, D.; Heibel, C.; Bandermann, F. *Des. Monomers Polym.* **1998**, *1*, 285.
- (13) Broska, D.; Fieberg, A.; Bandermann, F. *Des. Monomers Polym.* **1998**, *1*, 37.
- (14) Maurer, A.; Dissertation, Universität Mainz, Mainz, Germany, 1998.
- (15) Zhuang, R.; Müller, A. H. E. *Macromolecules* **1995**, *28*, 8043.

MA991575N